J. Coat. Technol. Res., **16** (5) 1367–1378, 2019
https://doi.org/10.1007/s11998-019-00219-0

Electrophoretic deposition of waterborne ultraviolet (UV)-curable coatings based on microgels

Junhua Chen, Teng Yuan, Weiping Tu, Kaimei Peng, Jianqing Hu, Feng Wang

Abstract Microgels are novel functional polymers with an intramolecular crosslinked structure that can significantly improve the mechanical properties of coatings. We demonstrate herein for the first time successful fabrication of microgels based on branched poly(ethylenimine) (PEI) and their incorporation into water-soluble polyacrylate (WPA), with subsequent preparation of compact coatings via electrophoretic deposition (EPD) and ultraviolet (UV) radiation. The films including the microgels exhibited tensile strength and elongation at breakage values above 6.82 MPa and 72.09%, respectively. The coatings showed good thermal stability, decreased water absorption, outstanding durability, and rust resistance after immersion in 5 wt% NaCl solution for 7 days at 40°C. This work provides a new strategy that can be readily applied to a variety of conductive substrates.

Keywords Microgels, Branched poly(ethylenimine), Electrophoretic deposition, UV radiation, Tensile strength

J. Chen, W. Tu (✉), J. Hu, F. Wang
School of Chemistry and Chemical Engineering, South China University of Technology, 381 Wushan Road, Tianhe District, Guangzhou 510641, China
e-mail: cewptu@yeah.net

J. Chen
e-mail: cehjchen@yeah.net

J. Hu
e-mail: glennhu@scut.edu.cn

F. Wang
e-mail: fengwang@scut.edu.cn

T. Yuan
College of Materials and Energy, South China Agricultural University, 483 Wushan Road, Tianhe District, Guangzhou 510642, China
e-mail: yuant@scau.edu.cn

K. Peng (✉)
School of Chemistry and Chemical Engineering, Qiannan Normal University for Nationalities, Duyun 558000, China
e-mail: scutpkm@163.com

Introduction

Microgels comprise a water-swollen, microscopic three-dimensional crosslinked network of polymeric particles dispersed in a suitable solvent, representing a special class of colloid with properties such as stability over a longer period of time, kinetically stable structure held together by covalent bonding (or other strong forces), tunable architecture, high porosity, and adjustable dimensions.[1–3] Microgels have many potential applications as so-called smart colloids due to their reversible swelling and deswelling characteristics and ability to respond to external changes, e.g., in temperature, pH, electrochemical stimulus, pressure, and external fields.[4–8] Their versatility in terms of size, functionality, and mechanical properties makes them potential candidates for use in drug or gene delivery and tissue engineering, and as biointerface materials.[9]

Microgel networks exhibit high mechanical strength and water-holding capacity, which is attributed to the presence of numerous hydrophilic and crosslinkable functional groups.[2] Furthermore, incorporation of microgels into coatings can improve their rheological properties, dispersion stability, and chemical resistance. Research interest has recently been drawn to synthesis of thermoresponsive microgels by controlling the crosslinking of poly-(*N*-isopropylacrylamide).[3,10–15] Hyperbranched polymers have also attracted increased attention in recent years due to their various unique properties, such as relatively simple processing at low

cost, low viscosity, high activity, and tailorable compatibility.[16,17] Well-defined microparticles with hyperbranched polymer (methacrylated hyperbranched polyglycerol, HyPG-MA) of uniform size can also be used for drug delivery and tissue engineering.[18] Microgels with hyperbranched polymer can be used not only for biomedical applications, but also for industrial coatings.[11] However, such use of microgels to fabricate waterborne UV-curable EPD coatings with tunable patterns has rarely been described.[9,19,20]

Electrophoretic deposition (EPD) can be widely used to produce coatings on conductive substrates with various shapes in a cost-effective manner.[21–24] However, more importantly, EPD techniques represent environmentally friendly and tunable methods for fabrication of uniform coatings by simple adjustment of the deposition time and applied potential.[22,25,26] Water-based UV-curing systems have been applied in the field of electrophoretic coatings to address the limitation of the high temperature required for thermal curing of electrophoretic coatings, guiding the development of EPD processes.[27,28]

In the work presented herein, we prepared novel waterborne UV-curable electrophoretic deposition coatings based on microgels with hyperbranched polymer. We studied the chemical structure of the microgels and their dispersibility in aqueous solution. The properties of the coatings including their thermal stability, mechanical properties, water absorption, corrosion resistance, and other physical properties were investigated. This study therefore describes a promising strategy for preparation of UV-curable EPD coatings.

Materials and methods

Materials

Butyl acrylate (BA, ≥ 99.5%), methyl methacrylate (MMA, ≥ 99.5%), 2-(dimethylamino)ethyl methacrylate (DMAEMA, ≥ 99.5%), 2-hydroxypropyl methacrylate (HPMA, ≥ 99.5%), 2-hydroxyethyl acrylate (HEA, ≥ 96%), styrene (St), and 2,2′-azobis(2-methylpropionitrile) (AIBN, ≥ 98%) were purchased from Aladdin Chemical Ltd. (Shanghai, China) and used with further purification. 3-Isocyanatomethyl-3,5,5-trimethylcyclohexyl isocyanate (IPDI, purity > 99.5%, NCO% ≥ 37.5%) was purchased from Bayer Co., Ltd. (China). Branched poly(ethylenimine) (PEI, ≥ 99%, $M_w = 2.5 \times 10^4$ g/mol and $M_n = 1.0 \times 10^4$ g/mol, Fig. 1) was purchased from Sigma-Aldrich. 3-Glycidyloxypropyltrimethoxysilane (KH560, ≥ 98%, Fig. 1) was supplied by SICO Performance Material (Shandong) Co., Ltd. Dibutyltin dilaurate (DBTDL, ≥ 99.5%) and 2,6-di-*tert*-butyl-*p*-cresol (DBHT, ≥ 99.5%) were purchased from Macklin and used as catalyst and polymerization inhibitor, respectively. 2-Hydroxy-2-methyl-1-phenyl-1-propanone (Darocur 1173, ≥ 99.5%) was purchased from Aldrich and used as photoinitiator. All other solvents were distilled under reduced pressure prior to use and received from Sinopharm Chemical Reagent Co. Ltd., China.

Synthesis of acrylate prepolymer

WPA was prepared by the following procedure (Fig. 1): IPDI (10.01 g, 0.045 mol), DBTDL (4 mg), and DBHT (71.8 mg) were dissolved in ethyl acetate (5 mL) in a three-necked, round-bottomed flask with dry nitrogen atmosphere. The temperature was increased to 60°C. HEA (5.44 g, 0.045 mol) was added into this polymer solution after about 1 h. Polymerization was allowed to continue for another 2 h. It was assumed that NCO-terminated unsaturated monomer (IPDI-HEA, Fig. 1) was successfully prepared.[29]

In the second step, the synthesis was carried out in a three-necked, round-bottomed flask equipped with a mechanical stirrer, dropping funnel, and reflux condenser. DMAEMA (15.0 mL), MMA (26.0 mL), BA (34.0 mL), HPMA (26.0 mL), St (10 mL), and AIBN (2.0 g) were dissolved in 2-acetoxy-1-methoxypropane (PGMEA, 43.5 mL) in the dropping funnel to prepare mixed solution. The four-necked round-bottom flask (500 mL) at room temperature bearing PGMEA (10.3 mL) was purged under nitrogen gas flow for 30 min then subsequently heated to 80°C. Then, the mixed solution was dropped slowly into the reactor during 3 h. The reaction was allowed to continue for another 12 h. The crude reaction mixture was at 65% yield.

In the third step, IPDI-HEA, DBTDL (0.01 wt%), and DBHT (0.5 wt%) were dissolved in PGMEA (5 mL) in a flask at room temperature, then added dropwise into the above crude reaction mixture over a period of 1 h at 60°C. When the peak at 2260 cm^{-1} for NCO groups completely disappeared, acrylate prepolymer was obtained. This prepolymer was finally cooled to 50°C and neutralized using 2-hydroxypropanoic acid.

Synthesis of microgels with hyperbranched structure

Microgel solution was synthesized in three steps following the procedures shown in Fig. 2. PEI (2.58 g) and KH560 (4.68 g) were mixed in 30 mL tetrahydrofuran in a 100-mL reaction flask filled with N_2. Under room temperature, the reaction was continued for an additional 12 h. PEI-KH560 graft polymer (abbreviated as PIK) was obtained as clear liquid (Fig. 2a). After addition of acetic acid (2.63 g), the mixture was left to neutralize for 1 h at 40°C with stirring (Fig. 2b). Then, 66 mL deionized water was added dropwise within 2 h, and the temperature was kept constant at 60°C, resulting in microgel solution with solid content of 15% (Fig. 2c).

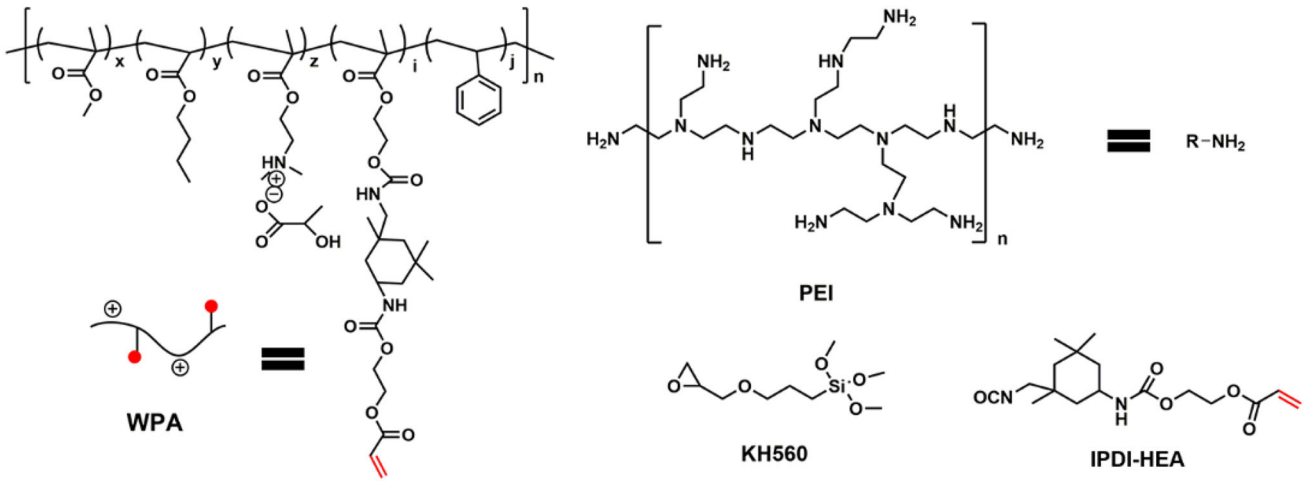

Fig. 1: Chemical structures of WPA, PEI, KH560, and IPDI-HEA

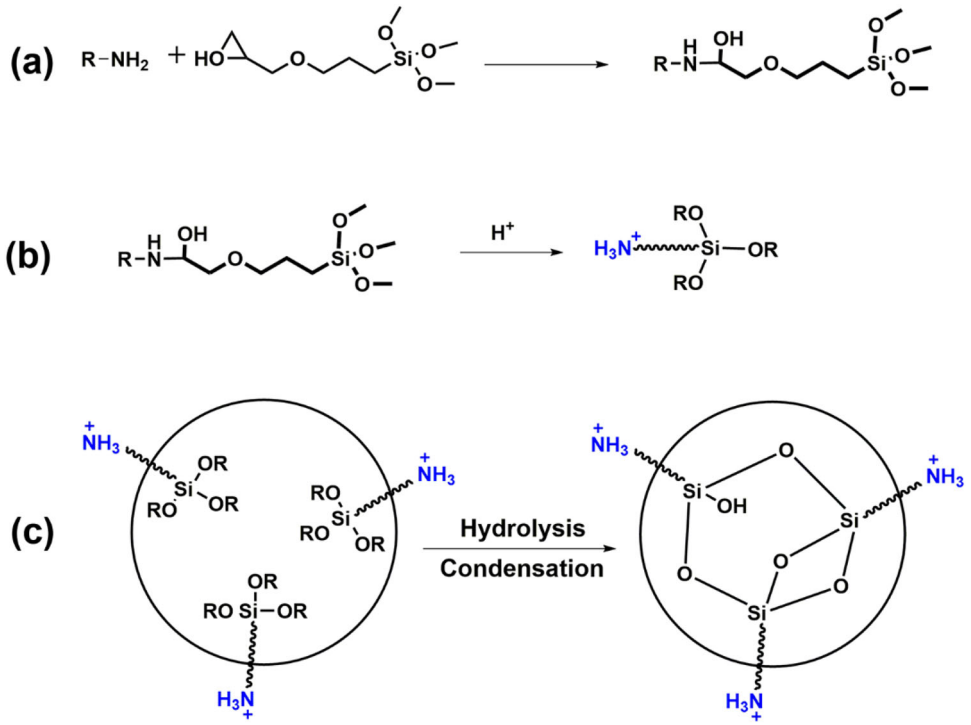

Fig. 2: Synthesis of microgels with PEI

Preparation of UV-curable EPD coatings

Waterborne UV-curable EPD coatings were prepared via the procedure illustrated in Fig. 3. The prepared acrylate prepolymer, the microgel solution (5 wt% or 15 wt% to pure acrylate prepolymer), Darocur 1173 (5 wt%), and distilled water were mixed together with rapid stirring for 30 min to obtain an aqueous emulsion (named WPA-PIK) with solid content of 15%. Tin plate after phosphating treatment was used as cathode, and aluminum alloy panel plate as anode. The distance between the two plates was 10 cm. Electrophoresis was carried out at 80 s at an applied voltage of 50 V, depositing coatings on the surface of the cathode plate. The coated plates were then rinsed with deionized water and placed in an oven for 10 min at 80°C to remove moisture. The plates were exposed to 1000 W UV radiation for 90 s.

Characterization

Fourier-transform infrared (FTIR) spectra of all the polymers and monomers were obtained over the

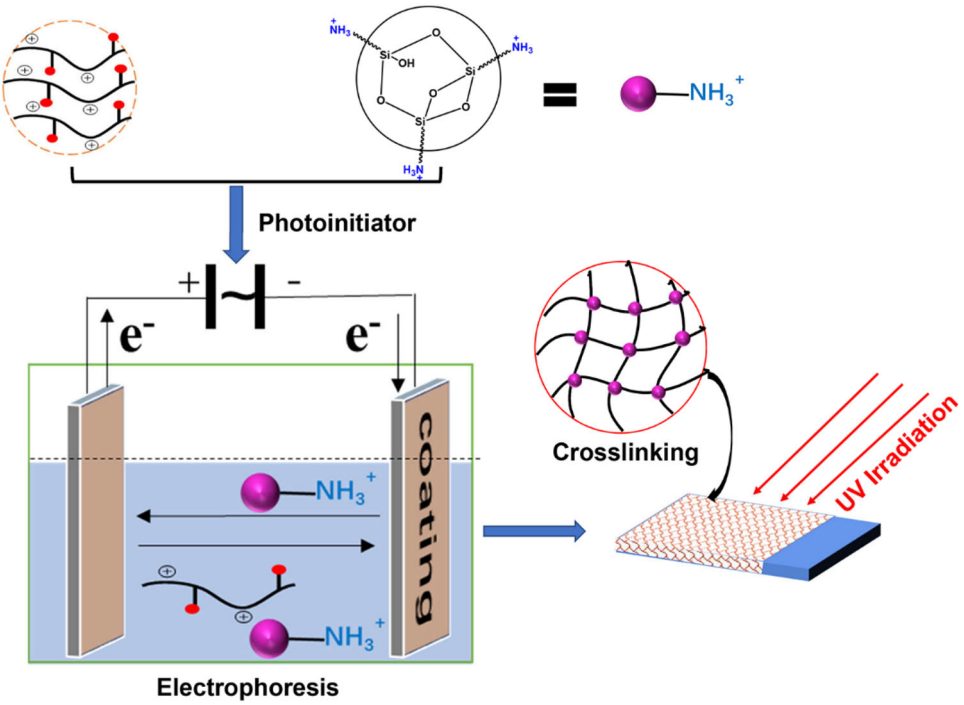

Fig. 3: Illustration of UV-curable EPD protocol

wavenumber range of 4000 to 400 cm^{-1} using a Bruker VERTEX 70 with KBr pellets. ^{1}H nuclear magnetic resonance (^{1}H NMR) spectra were recorded using a Bruker AVANCE III HD 400 spectrometer with $CDCl_3$ as solvent.

Dynamic light scattering (DLS) measurements of aqueous polymer solutions (15 wt%) were carried out using a laser light scattering spectrometer (ALV-5000, Langen, Germany) equipped with a multi-τ digital time correlater. Light (λ = 632.8 nm) from a solid-state He–Ne laser (22 mW) was used as the incident beam. The measurements were performed at a scattering angle of 90°C. The correlation function was analyzed via the Contin method.[30,31]

Differential scanning calorimetry (DSC) was carried out using a DSC 200F3 (Netzsch, Germany). Under nitrogen condition, dry specimens of 5–10 mg were sealed in aluminum pans and heated from 25 to 150°C at 10°C min^{-1} to eliminate thermal history. Then, a new thermal cycle was applied from −70 to 250°C at 10°C min^{-1} to evaluate the glass-transition temperature (T_g). Thermogravimetric analysis (TGA) was performed using a Netzsch TG209F3 instrument. The samples were heated from 30 to 600°C at rate of 10°C min^{-1} under N_2 atmosphere.

Scanning electronic microscopy (SEM) of untreated as well as treated specimens was carried out using a JEOL JXA-840A with electron probe microanalysis (Japan) at accelerating voltage of 10 kV. The specimens were sputter-coated with 150 Å gold (Edwards coater), then inspected at magnification range of 35–10,000 to detect surface morphological changes.

The tensile properties of sample specimens were measured using a multifunctional electronic strength tester TS2000-S (Taiwan). The sample bars (7×80 mm^2) were cut to thickness of 0.4–0.8 mm. Standard tensile testing was performed in accordance with ASTM 412-83 methods. The tensile strength, Young's modulus, and elongation at breakage were measured at 10 mm/min and room temperature.[32,33]

The glossiness (in gloss units of ''Gs'') of coatings was measured using an IG-330 gloss meter (Horiba, Japan) in accordance with standard ISO 2813 protocol.[34] The coated substrate was illuminated by a red diode laser (650 nm) at an angle of 60°.[35] The glossiness was obtained as the average of at least five replicates. The hardness of the coating was graded according to ASTM protocol D3363 using a set of Faber Castell 9000 pencils (Derwent's) from 9B to 9H held against the coating surface at an angle of 45° and pushed away from the operator. All pencils were sharpened and then flattened by rubbing on abrasive paper (3M, grit no. 400) at an angle of 90° to create a flat, smooth, and circular cross section.[36,37] The adhesion of the coatings was tested using the crosscut method in accordance with ASTM D3359 standard.[38] The surface of coatings was cut with a blade. The distance between each line was 2 mm. A piece of 3M 250 masking tape was then pressed onto the coatings and quickly peeled off. The number of tiny squares removed with the adhesive tape was then calculated.[36] A membrane impacting tester (QCJ-50, Shanghai Modern Environmental Engineering Technology, China) was employed to measure the effect of impact on

the adherence of the coatings. The coated tin sample was placed directly below the impact hammer (1000 ± 1 g), Which fell down from a height of 50 cm to impact on the coatings. The coating flexibility of a prepainted sheet was measured using a QTX tester (Tianjing Jingkelian Material Testing Machine Co., LTD) according to ASTM D4145. During fabrication into products, precoated sheets are subjected to stresses by brake bending, which could exceed the flexibility of the coating, resulting in its fracture and exposing the substrate, or in loss of adhesion of the coating to the substrate. This test was used to evaluate the ability of the coating system to withstand such stresses during fabrication. The salt spray test was conducted in harsh chemical environment according to ASTM B-117 standard. Coated tin plates were immersed in 5 wt% NaCl salt solution with pH between 6.5 and 7.2 at 40°C for 7 days.[39–41] The water absorption (WS) of the samples was calculated as

$$\text{Water absorption percentage} = \frac{W_2 - W_1}{W_1} \times 100\%, \quad (1)$$

where W_2 and W_1 are the masses of the film after swelling in water for 72 h and the original dry film, respectively.[42]

Results and discussion

FTIR and ^{1}H NMR analyses of PIK monomer

Figure 4 shows the FTIR spectrum of the PIK monomer. The broad peak at 3364.4 cm^{-1} corresponds to hydroxyl stretching absorption of amine groups, indicating the possibility that the primary amine in PEI underwent a ring-opening reaction with the epoxides. The peaks at 2937.7 and 2837.5 cm^{-1} derive respectively from asymmetric and symmetric stretching vibration of C–H in $–CH_3$ and $–CH_2–$.[33] The typical bands located at 1659, 1352, and 1202 cm^{-1} can be assigned to absorption due to N–H stretching, C–N stretching, and symmetric stretching of C–O–C in $CH_2–O–CH_2$ of KH560. The broad strong peaks near 1107 cm^{-1} correspond to asymmetric vibration of Si–O–C, and the stretching peaks at ~ 838 cm^{-1} to bending vibration of Si–C, indicating the occurrence of a reaction between KH560 and PEI in the system.

Figure 5 shows the ^{1}H NMR spectrum of the PIK monomer. The peak at 6.01 ppm corresponds to epoxy group generating hydroxyl groups after ring-opening. The weak peak at 5.52 ppm corresponds to proton of N–H group. The peak at 4.52 ppm corresponds to the proton of –CH– group next to hydroxyl group. The characteristic peaks at 3.04–3.75 ppm are assigned to methyl, methylene, and methine protons on different alkyl chains of PIK. The peaks at 2.45–2.73 ppm correspond to proton of $–CH_2–$ group. The strong peak at 1.89 ppm corresponds to other N–H groups in the structure. The weak peaks at 1.53 and 0.59 ppm correspond to other methylene protons. These ^{1}H NMR and FTIR spectra confirm successful synthesis of the target monomer PIK.

Particle size control of WPA-PIK emulsions

Figure 6 shows the average particle size distribution (as determined by dynamic light scattering) and size distribution of aqueous solutions containing pure WPA, WPA-PIK5% (5 wt% of PEI-KH560 to pure acrylate prepolymer), and WPA-PIK15% (15 wt% of PEI-KH560 to the pure acrylate prepolymer). For the WPA solution, the average particle size was found to be 43.8 nm, due to ionizable groups arising from DMAEMA units. In the case of mixed aggregates formed by WPA and microgel solution, PIK and WPA were mixed well and dispersed in water. The particle size of WPA-PIK was found to be clearly split into two different peaks, at 37.8 nm (assigned to WPA) and

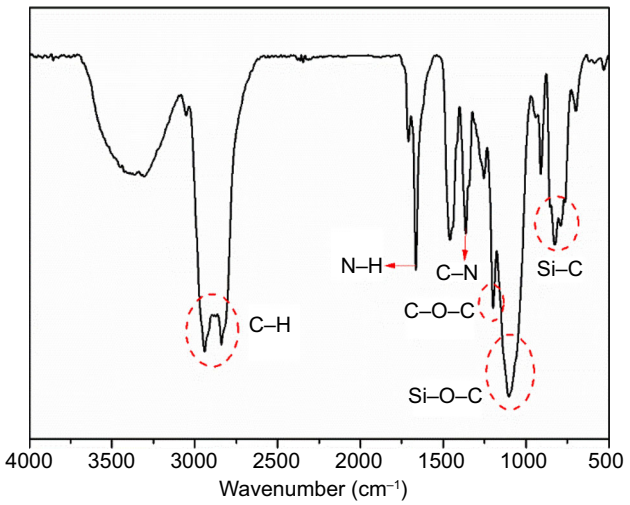

Fig. 4: FTIR spectrum of PIK monomer

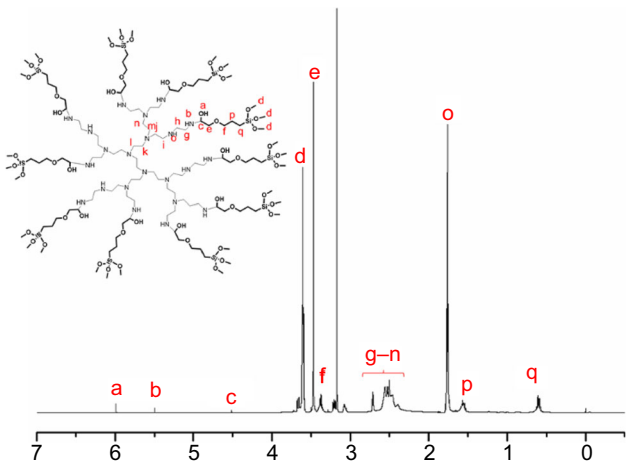

Fig. 5: ^{1}H NMR spectrum of PIK monomer

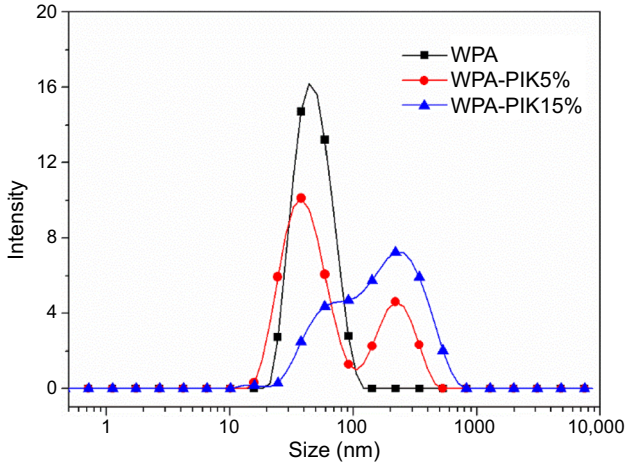

Fig. 6: Particle size distribution of WPA-PIK emulsions with different mass ratios

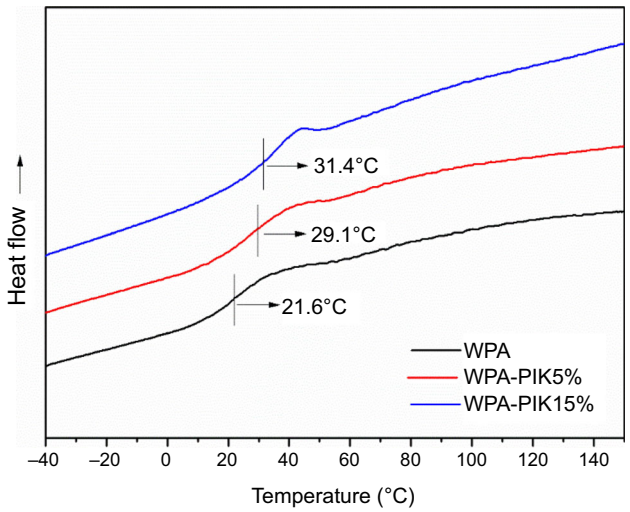

Fig. 7: DSC curves of different EPD coatings

220 nm (assigned to microgel solution). For WPA-PIK15%, it may be that the microgel formed the central core of mixed aggregates due to the much higher content of PIK, provoking water repellency, while the ionizable groups in WPA were left on the surface to obtain a stable state.[43]

Thermal stability of waterborne UV-curable EPD coatings

The DSC curves of the coatings obtained using PIK monomer are shown in Fig. 7, revealing T_g values of 21.6, 29.1, and 31.4°C for WPA, WPA-PIK5%, and WPA-15%, respectively. For pure WPA, the measured T_g is close to the theoretical value of 20°C. The T_g values of the WPA-PIK samples were higher than that of pure WPA, which can probably be attributed to incorporation of the microgel solution containing compact hyperbranched segments and $(–C–Si–O–)_n$ chains.[44] A broad glass transition was seen for WPA-PIK in the range of 20–60°C, which can be attributed to the remarkable phase separation of soft and hard segments in the hyperbranched structure.[45] WPA-PIK15% showed a higher T_g value due to hydrogen bonding arising when the strained ring structure in KH560 was converted to an open chain structure. Hydroxyl protons would form hydrogen bonds with nitrogen of the Mannich bridge as well as with adjacent hydroxyl groups, causing both inter- and intramolecular hydrogen bonding.[46,47]

The TGA curves and corresponding derivative weight loss curves (DTG) of the waterborne UV-curable EPD coatings obtained in N_2 are shown in Figs. 8a and 8b, respectively, while the temperature of maximum mass loss rate (T_{max}) and char yield (Y_c) are summarized in Table 1. All the coatings lost < 5% of their initial weight at around 100°C due to removal of nonvolatile solvent and evolution of water. All the

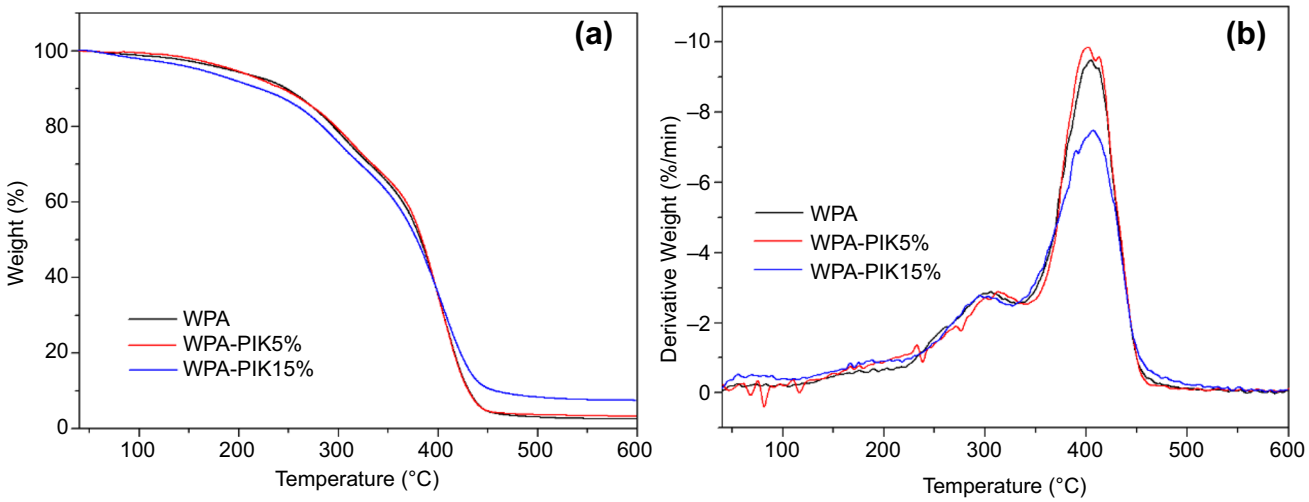

Fig. 8: TGA curves (a) and corresponding DTG curves (b) of waterborne UV-curable EPD coatings with varying contents of PIK monomer

samples exhibited a similar thermal decomposition profile. The first stage of weight loss in the temperature range of 250–350°C can be attributed to degradation of urethane groups in WPA. The second stage of weight loss, observed within the range of 350–440°C, probably relates to degradation of ester bonds in polyester urethanes and imide structures of PEI.[48,49] However, WPA-PIK15% exhibited the lowest T_{max1} of 295°C and the highest T_{max2} of 406.6°C. The reason is that WPA-PIK15% mainly contained more hyperbranched structures, and might form a certain encapsulation of the core–shell structure, as confirmed in Fig. 6. WPA-PIK5% and WPA-PIK15% based on PEI-KH560 exhibited char yield of 3.26 and 7.17 wt% at 600°C. The microgels probably contained significant amounts of hydrogen bonds, forming a highly crosslinked network structure. In addition, terminal groups of PIK had stable Si–O structure. Accordingly, the thermal stability of the EPD coating was enhanced by increased addition of microgel.

Table 1: Thermal stability of waterborne UV-curable EPD coatings

Formulation	T_{max1} (°C)	T_{max2} (°C)	Y_c at 600°C (%)
WPA	306.4	404.3	2.52
WPA-PIK5%	311.3	401.4	3.26
WPA-PIK15%	295.0	406.6	7.17

Mechanical properties and water resistance

Figure 9 illustrates typical stress–strain curves of waterborne UV-curable EPD coating films with different PIK contents, obtained from tensile measurements; the details are presented in Table 2. All the films behaved as weak elastomers without a distinct yield stress point. The tensile strength decreased from 3.44 to 1.39 MPa when the PIK content was lower than 5%, followed by a sharp increase with further increase in the PIK content to 15%. It can also be seen from these curves that the elongation at breakage increased rapidly from 37.04 to 88.18% with 5% PIK addition, but then decreased to 72.09%.[50] WPA-PIK15% showed the highest tensile strength and Young's modulus. All these results can be explained by the uniform dispersibility of the microgel solution in the system, the enhanced interfacial adhesion due to the large number of intramolecular hydrogen bonds, and the hyperbranched structure of PEI that enhances the toughness of the material.[51]

Figure 10 shows the water absorption behavior of the coatings with various PIK contents after 72 h. According to these results, the water absorption values decreased from 5.74 to 0.94 wt% with increasing PIK

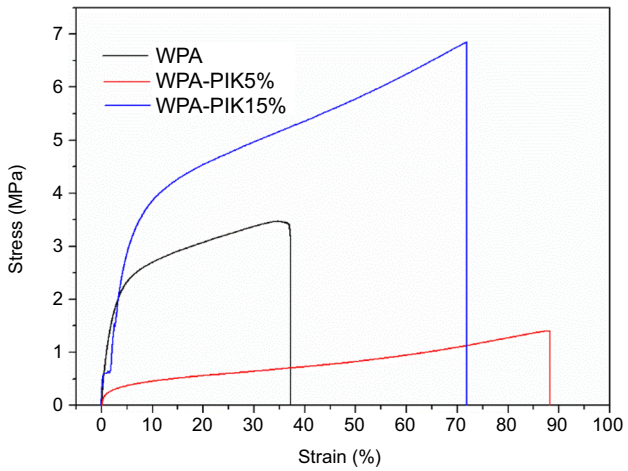

Fig. 9: Stress–strain curves of EPD films with different PIK contents

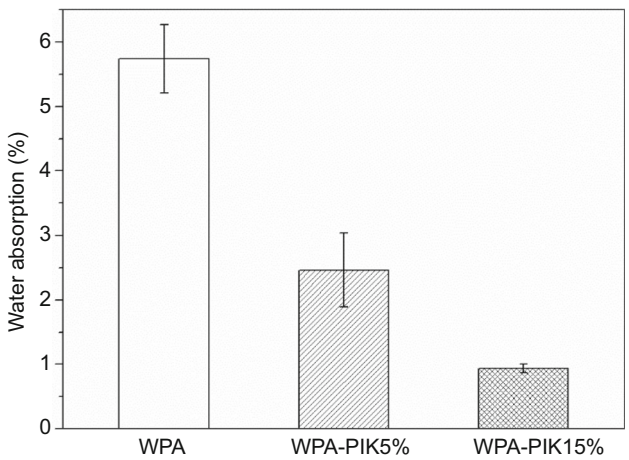

Fig. 10: Water absorption properties of films with varying PIK contents at room temperature after 72 h

Table 2: Detailed data from tensile measurements

Formulation	Tensile strength (MPa)	Elongation at breakage (%)	Young's modulus (MPa)
WPA	3.44	37.04	9.29
WPA-PIK5%	1.39	88.18	1.58
WPA-PIK15%	6.82	72.09	9.46

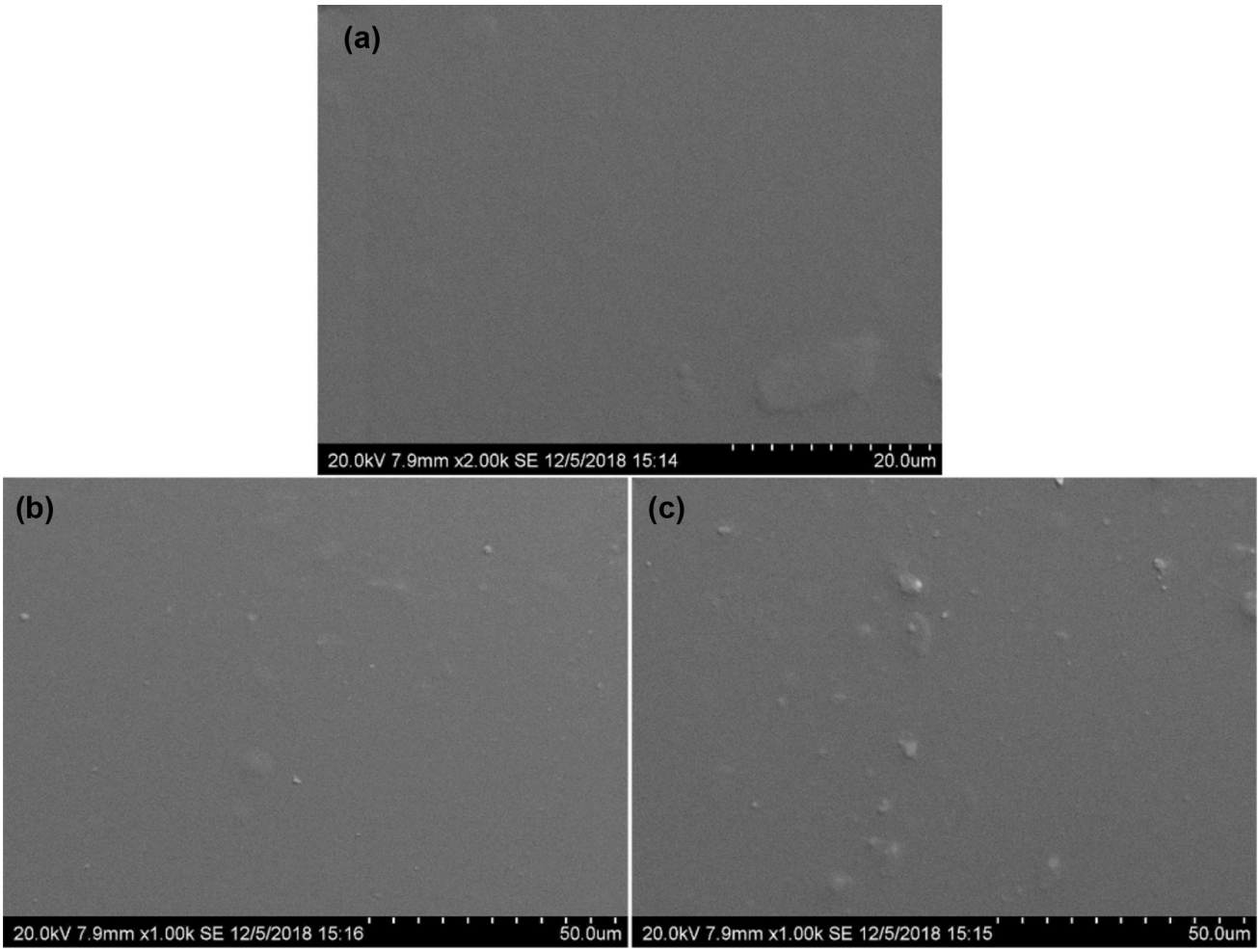

Fig. 11: SEM images of films with varying PIK contents: (a) WPA at 20.0 μm scale, (b) WPA-PIK5% at 50.0 μm scale, and (c) WPA-PIK15% at 50.0 μm scale

Table 3: General performance of waterborne UV-curable EPD films

Formulation	Thickness (μm)	Pencil hardness	Glossiness (Gs)
WPA	30	2H	92.0
WPA-PIK5%	32	2H	34.7
WPA-PIK15%	31	3H	16.3

content. The crosslinking between polyacrylate and hyperbranched structure was enhanced with incorporation of the PIK monomer, forming inorganic–organic networks, which was beneficial to increase the water resistance.[50] Furthermore, migration of silicon atoms on the surface of the films could decrease their surface energy and enhance their water resistance.

Other physical properties of UV-curable EPD coatings

The surface morphology of the UV-curable EPD coatings, both untreated and treated with PIK emulsion, as observed by SEM is shown in Fig. 11 to reveal the variation in the surface of the coatings. As shown in Fig. 11a, the surface of the pure WPA-coated film was smooth, revealing no phase separation or cracking. As illustrated in Figs. 11b and 11c, many tiny particles were observed on the surface of the coatings with PIK, indicating that the surface of the film was rough and uneven. The WPA and microgel solutions were two phases separated from each other, which is in line with Fig. 6, and the microgels also formed crosslinked particles to enhance the physical properties.

The overall performance of the UV-curable EPD films is presented in Table 3. The thickness of the coatings was about 30 μm. The pencil hardness of the

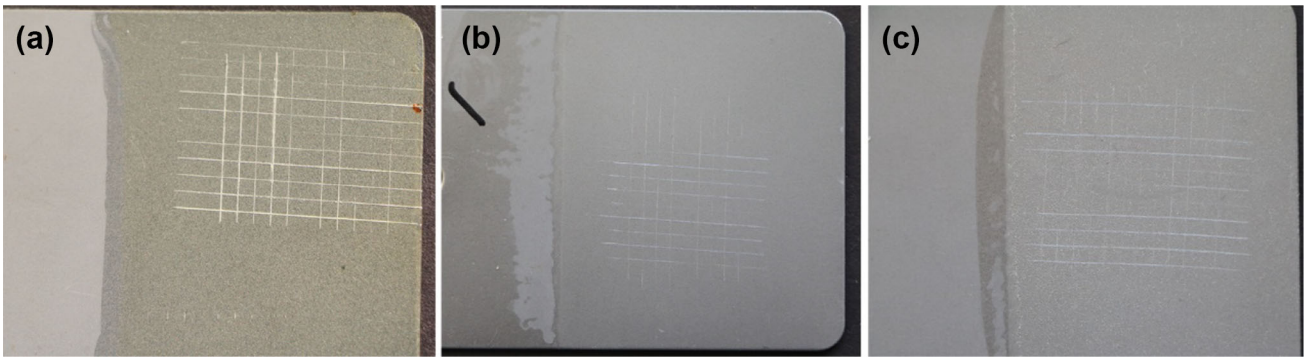

Fig. 12: Adhesion test results of UV-curable EPD coatings with varying PIK contents with phosphated plate as substrate, and separation between the lines of 2 mm: (a) WPA, (b) WPA-PIK5%, and (c) WPA-PIK15%

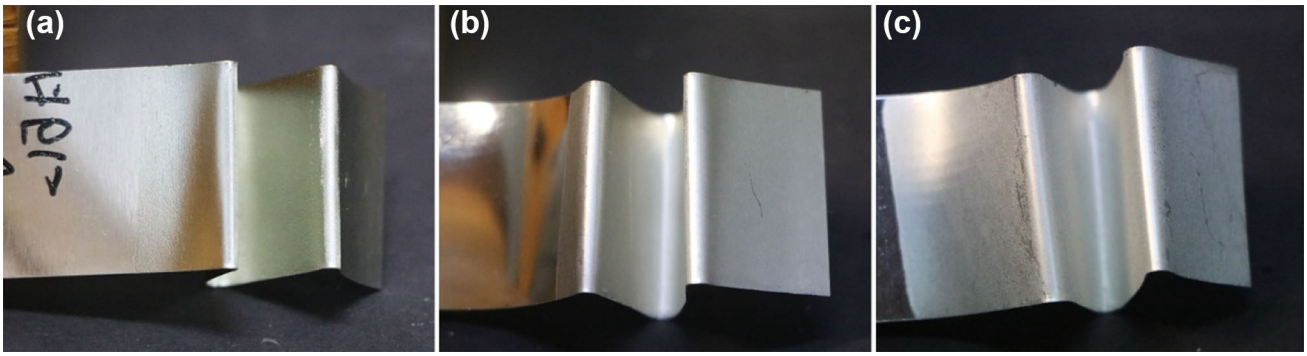

Fig. 13: Flexibility of UV-curable EPD coatings with varying PIK contents with tin plate as substrate, recorded after bending: (a) WPA, (b) WPA-PIK5%, and (c) WPA-PIK15%

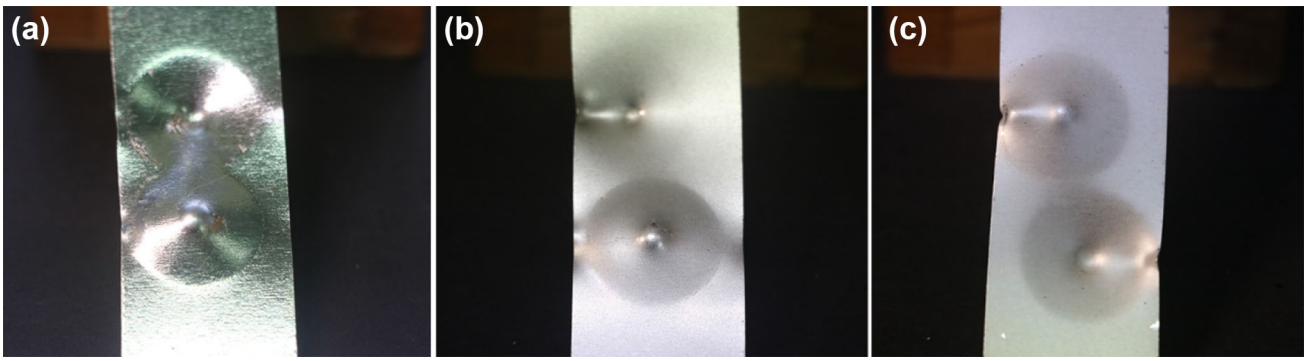

Fig. 14: Front and reverse of UV-curable EPD coatings with varying PIK contents on tin plate after impact: (a) WPA, (b) WPA-PIK5%, and (c) WPA-PIK15%

coating was increased slightly from 2H to 3H, which can be attributed to the crosslinked particles in the microgel solution. However, these outstanding mechanical properties were achieved at the expense of a reduction in the glossiness of the coatings, which increased in the presence of monomers (St, methyl methacrylate, etc.).[52] When the amount of crosslinked microgels in the coating exceeded a certain value, minor cracking occurred on the surface, resulting in a relatively rough film.

The adherence of the UV-curable EPD coatings measured according to ASTM D3359 standard is shown in Fig. 12. Since no evidence of detachment from the substrate was found after this test, the films exhibited excellent adherence, reaching the top ranking of 5B on this scale.[38] It is well known that more polar groups in a crosslinking system may benefit its adhesion to a substrate by increasing the adhesive force.[53,54] The hydroxyl groups and hyperbranched structure of the microgels undoubtedly promoted the

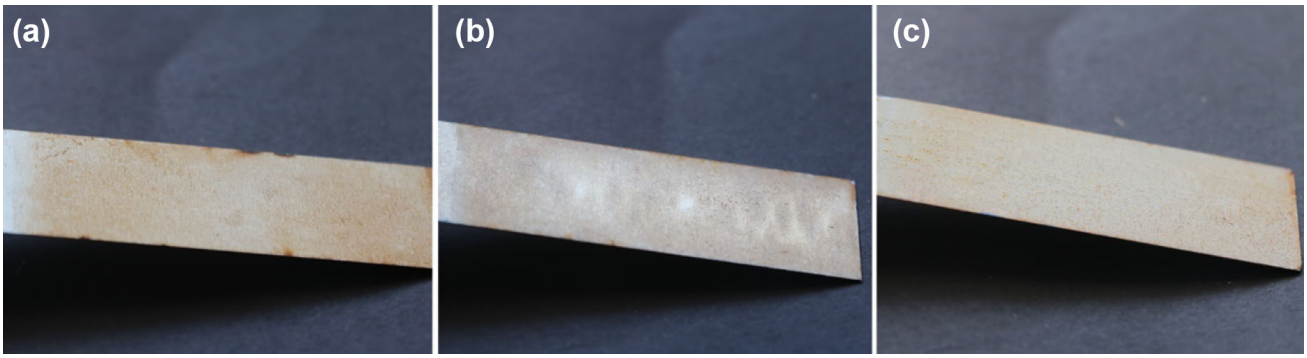

Fig. 15: Surface of corroded UV-curable EPD coatings with varying PIK contents: (a) WPA, (b) WPA-PIK5%, and (c) WPA-PIK15%

adhesion. However, there was a slight decrease in the flexibility of WPA-PIK15% (Fig. 13). These results are attributed to the increased crosslink density and rigidity due to the lack of flexible chains.[55] The impact resistance results for the UV-curable EPD coatings with varying PIK contents, coated on tin plate as a substrate and subjected to quick impact damage, on both the front and reverse, are shown in Fig. 14. These results indicate no influence on the adherence of the coating to the substrate or rupture to any noticeable degree.

The results of the harsh corrosion resistance study conducted on UV-curable EPD coatings with varying PIK contents for 7 days are shown in Fig. 15. A tin plate bearing coated sections was immersed in 5 wt% NaCl solution with pH between 6.5 and 7.2 at 40°C, and a photograph of the surface was taken after removal from the solution. The coatings with pure WPA prepared via EPD were found to be deteriorated after the corrosion test.[30] As shown in Figs. 15b and 15c, coating of WPA-PIK5% on the tin plate showed negligible degradation after the corrosion test, with no visible evidence of rust on the region coated with WPA-PIK15%. This enhanced corrosion resistance can be attributed to the strong crosslinking network and partially hydrophobic polar groups of the microgel.

Conclusions

Microgels with PEI were fabricated by addition reaction, then incorporated into pure acrylic WPA after acidification hydrolyzation. Increasing the content of PIK in EPD yielded separated larger particles with size of 220 nm. The coating was prepared via aqueous EPD and UV radiation. After addition of the microgel, the coatings showed a wider range of glass-transition temperatures, good thermal stability, and decreased water absorption. According to tensile measurements, the tensile strength and elongation at breakage were greatly enhanced. According to SEM images and glossiness testing, the excellent adhesion, outstanding impact tolerance, and bending resistance of the coatings were achieved at the cost of some properties due to the phase separation. Tin plates coated with WPA-PIK15% did not rust after immersion in 5 wt% NaCl solution for 7 days. This facile method for coating of conductive substrates will have promising applications.

Acknowledgments This work was financially supported by the Natural Science Foundation of Guangdong Province (Grant Nos. 2018A030313483, 2018A030313235 and 2018A030310349), Foundation for High-Level Talents in Qiannan Normal University for Nationalities (qnsyrc201706), Guangzhou City Science and Technology Program (201803030003), and Research Fund Program of Guangdong Provincial Key Lab of Green Chemical Product Technology (GC201813).

References

1. Agrawal, G, Agrawal, R, ‘‘Stimuli-Responsive Microgels and Microgel-Based Systems: Advances in the Exploitation of Microgel Colloidal Properties and Their Interfacial Activity.’’ *Polymers*, **10** (4) (2018)
2. Farjami, T, Madadlou, A, ‘‘Fabrication Methods of Biopolymeric Microgels and Microgel-Based Hydrogels.’’ *Food Hydrocolloids*, **62** 262–272 (2017)
3. Dickinson, E, ‘‘Microgels—An Alternative Colloidal Ingredient for Stabilization of Food Emulsions.’’ *Trends Food Sci. Technol.*, **43** (2) 178–188 (2015)
4. Plamper, FA, Richtering, W, ‘‘Functional Microgels and Microgel Systems.’’ *Acc. Chem. Res.*, **50** (2) 131–140 (2017)
5. Chen, S, Peng, Y, Wu, Q, Chang, A, Qu, A, Shen, J, Xie, J, Farooqi, ZH, Wu, W, ‘‘Synthesis and Characterization of Responsive Poly(Anionic Liquid) Microgels.’’ *Polym. Chem.*, **7** (34) 5463–5473 (2016)
6. Farooqi, ZH, Khan, HU, Shah, SM, Siddiq, M, ‘‘Stability of poly(*N*-isopropylacrylamide-co-acrylic Acid) Polymer Microgels Under Various Conditions of Temperature, pH and Salt Concentration.’’ *Arab. J. Chem.*, **10** (3) 329–335 (2017)
7. Naseem, K, Begum, R, Wu, W, Irfan, A, Farooqi, ZH, ‘‘Advancement in Multi-Functional Poly(styrene)-Poly(*N*-

isopropylacrylamide) Based Core-Shell Microgels and Their Applications.'' *Polym. Rev.*, **58** (2) 288–325 (2018)
8. Naseem, K, Begum, R, Wu, W, Usman, M, Irfan, A, Al-Sehemi, AG, Farooqi, ZH, ''Adsorptive Removal of Heavy Metal Ions Using Polystyrene-Poly(*N*-isopropylmethacrylamide-Acrylic Acid) Core/Shell Gel Particles: Adsorption Isotherms and Kinetic Study.'' *J. Mol. Liq.*, **277** 522–531 (2019)
9. Kodlekere, P, Pich, A, ''Functional Microgels for the Decoration of Biointerfaces.'' *ChemNanoMat*, **4** (9) 889–896 (2018)
10. Pelton, R, Chibante, P, ''Preparation of Aqueous Latices with *N*-Isopropylacrylamide.'' *Colloids Surf.*, **20** (3) 247–256 (1986)
11. Begum, R, Naseem, K, Farooqi, ZH, ''A Review of Responsive Hybrid Microgels Fabricated with Silver Nanoparticles: Synthesis, Classification, Characterization and Applications.'' *J. Sol-Gel Sci. Technol.*, **77** (2) 497–515 (2016)
12. Begum, R, Farooqi, ZH, Khan, SR, ''Poly(*N*-isopropylacrylamide-acrylic Acid) Copolymer Microgels for Various Applications: A Review.'' *Int. J. Polym. Mater. Polym. Biomater.*, **65** (16) 841–852 (2016)
13. Farooqi, ZH, Khan, A, Siddiq, M, ''Temperature-Induced Volume Change and Glucose Sensitivity of Poly[(*N*-isopropylacry-lamide)-co-Acrylamide-co-(Phenylboronic acid)] Microgels.'' *Polym. Int.*, **60** (10) 1481–1486 (2011)
14. Farooqi, ZH, Siddiq, M, ''Temperature-Responsive Poly(*N*-Isopropylacrylamide-Acrylamide-Phenylboronic Acid) Microgels for Stabilization of Silver Nanoparticles.'' *J. Dispersion Sci. Technol.*, **36** (3) 423–429 (2015)
15. Farooqi, ZH, Wu, W, Zhou, S, Siddiq, M, ''Engineering of Phenylboronic Acid Based Glucose-Sensitive Microgels with 4-Vinylpyridine for Working at Physiological pH and Temperature.'' *Macromol. Chem. Phys.*, **212** (14) 1510–1514 (2011)
16. Voit, BI, Lederer, A, ''Hyperbranched and Highly Branched Polymer Architectures-Synthetic Strategies and Major Characterization Aspects.'' *Chem. Rev.*, **109** (11) 5924–5973 (2009)
17. Zheng, Y, Li, S, Weng, Z, Gao, C, ''Hyperbranched Polymers: Advances from Synthesis to Applications.'' *Chem. Soc. Rev.*, **44** (12) 4091–4130 (2015)
18. Oudshoorn, MHM, Penterman, R, Rissmann, R, Bouwstra, JA, Broer, DJ, Hennink, WE, ''Preparation and Characterization of Structured Hydrogel Microparticles Based on Cross-Linked Hyperbranched Polyglycerol.'' *Langmuir*, **23** (23) 11819–11825 (2007)
19. Zhang, J, Yang, F, Shen, H, Wu, D, ''Controlled Formation of Microgels/Nanogels from a Disulfide-Linked Core/Shell Hyperbranched Polymer.'' *ACS Macro Lett.*, **1** (11) 1295–1299 (2012)
20. Mao, AS, Shin, J-W, Utech, S, Wang, H, Uzun, O, Li, W, Cooper, M, Hu, Y, Zhang, L, Weitz, DA, Mooney, DJ, ''Deterministic Encapsulation of Single Cells in Thin Tunable Microgels for Niche Modelling and Therapeutic Delivery.'' *Nat. Mater.*, **16** (2) 236–243 (2017)
21. Hu, RG, Zhang, S, Bu, JF, Lin, CJ, Song, GL, ''Recent Progress in Corrosion Protection of Magnesium Alloys by Organic Coatings.'' *Prog. Org. Coat.*, **73** (2–3) 129–141 (2012)
22. Besra, L, Liu, M, ''A Review on Fundamentals and Applications of Electrophoretic Deposition (EPD).'' *Prog. Mater. Sci.*, **52** (1) 1–61 (2007)
23. Cordero-Arias, L, Cabanas-Polo, S, Gilabert, J, Goudouri, OM, Sanchez, E, Virtanen, S, Boccaccini, AR, ''Electrophoretic Deposition of Nanostructured TiO_2/Alginate and TiO_2-Bioactive Glass/Alginate Composite Coatings on Stainless Steel.'' *Adv. Appl. Ceram.*, **113** (1) 42–49 (2014)
24. Boccaccini, AR, Zhitomirsky, I, ''Application of Electrophoretic and Electrolytic Deposition Techniques in Ceramics Processing.'' *Curr. Opin. Solid State Mater. Sci.*, **6** (3) 251–260 (2002)
25. Somarajan, S, Hasan, SA, Adkins, CT, Harth, E, Dickerson, JH, ''Controlled Electrophoretic Deposition of Uniquely Nanostructured Star Polymer Films.'' *J. Phys. Chem. B*, **112** (1) 23–28 (2008)
26. Van der Biest, OO, Vandeperre, L, ''Electrophoretic Deposition of Materials.'' *Annu. Rev. Mater. Sci.*, **29** (1) 327–352 (1999)
27. Patel, HV, Raval, J, Patel, P, ''Preparation and Performance of UV Curable Polyurethane Coating for Metal Surfaces.'' *Arch. Appl. Sci. Res*, **1** (2011) 294–305 (2009)
28. Zhang, Q, Huang, C, Wang, H, Hu, M, Li, H, Liu, X, ''UV-Curable Coating Crosslinked by a Novel Hyperbranched Polyurethane Acrylate with Excellent Mechanical Properties and Hardness.'' *RSC Adv.*, **6** (109) 107942–107950 (2016)
29. Liao, SR, Wei, Y, Zhang, YQ, Zhang, M, Feng, GF, ''Study on the Reaction of TDI and PPG with Organo-Tin Mixed Catalyst.'' *Adv. Mater. Res.*, **418–420** 13–17 (2012)
30. Yao, W, Wang, Z, Wu, X, Li, B, Zhong, X, Lin, J, Chen, J, Lai, Y, ''Preparation of Coatings from a Series of Silicone/Fluorine-Functionalized Polyacrylates via Electrophoretic Deposition.'' *Polym. Adv. Technol.*, **26** (9) 1148–1154 (2015)
31. Xu, W, Cai, X, Hao, A, Wang, J, ''Molecular Design of Brush-Like Amphiphilic Statistical Tripolymers and Their Self-Assembly Behaviors.'' *J. Chem. Eng. Data*, **58** (4) 927–931 (2013)
32. Yang, X, Shen, Y, Li, P, Li, G, ''Waterborne Cationic Fluorinated Polyurethane Modified by Perfluorinated Alkyl Long Chain.'' In: Bu, JL, Wang, PC, Ai, L, Sang, XM, Li, YG (eds.) *Appl. Eng. Mater.*, Pts 1–4, pp. 2116–2121 (2011)
33. Li, S, Yang, X, Huang, K, Li, M, Xia, J, ''Design, Preparation and Properties of Novel Renewable UV-Curable Copolymers Based on Cardanol and Dimer Fatty Acids.'' *Prog. Org. Coat.*, **77** (2) 388–394 (2014)
34. Standards, N, ''Paints And Varnishes—Determination Of Specular Gloss Of Non-metallic Paint Films At 20 Degrees, 60 Degrees and 85 Degrees.''
35. Wu, X, Liu, M, Zhong, X, Liu, G, Wyman, I, Wang, Z, Wu, Y, Yang, H, Wang, J, ''Smooth Water-Based Antismudge Coatings for Various Substrates.'' *ACS Sustain. Chem. Eng.*, **5** (3) 2605–2613 (2017)
36. Hu, H, Liu, G, Wang, J, ''Clear and Durable Epoxy Coatings that Exhibit Dynamic Omniphobicity.'' *Adv. Mater. Interfaces*, **3** (14) (2016)
37. Zheng, C, Liu, G, Hu, H, ''UV-Curable Antismudge Coatings.'' *ACS Appl. Mater. Interfaces*, **9** (30) 25623–25630 (2017)
38. Milionis, A, Dang, K, Prato, M, Loth, E, Bayer, I, ''Liquid Repellent Nanocomposites Obtained from One-Step Water-Based Spray.'' *J. Mater. Chem. A*, **3** (24) 12880–12889 (2015)
39. Calabrese, L, Proverbio, E, Bella, GD, Galtieri, G, Borsellino, C, ''Failure Behaviour of SPR Joints after Salt Spray Test.'' *Eng. Struct.*, **82** 33–43 (2015)
40. Hiromoto, S, ''Corrosion of Calcium Phosphate Coated AZ31 Magnesium Alloy under a Salt Spray Test.'' *Mater. Trans.*, **53** (4) 700–706 (2012)
41. Xue, B, Jiang, Y, Li, F, Xia, M, Sun, M, Liu, D, Zhang, X, Yu, L, ''Hydrophobic Modification of Dickite and Salt Spray Test Study on LLDPE/Modified Dickite Composite.'' *J. Appl. Polym. Sci.*, **116** (6) 3480–3488 (2010)

42. Peng, K, Zou, T, Ding, W, Wang, R, Guo, J, Round, JJ, Tu, W, Liu, C, Hu, J, ''Development of Contact-Killing Non-leaching Antimicrobial Guanidyl-Functionalized Polymers via Click Chemistry.'' *RSC Adv.*, **7** (40) 24903–24913 (2017)
43. Zhong, X-M, Wyman, I, Yang, H, Wang, J-B, Wu, X, ''Preparation of Robust Anti-smudge Coatings via Electrophoretic Deposition.'' *Chem. Eng. J.*, **302** 744–751 (2016)
44. Li, M, Liu, F, Li, Y, Qiang, X, ''Synthesis of Stable Cationic Waterborne Polyurethane with a High Solid Content: Insight from Simulation to Experiment.'' *RSC Adv.*, **7** (22) 13312–13324 (2017)
45. Asif, A, Hu, L, Shi, W, ''Synthesis, Rheological, and Thermal Properties of Waterborne Hyperbranched Polyurethane Acrylate Dispersions for UV Curable Coatings.'' *Colloid Polym. Sci.*, **287** (9) 1041–1049 (2009)
46. Rao, BS, Palanisamy, A, ''Monofunctional Benzoxazine from Cardanol for Bio-composite Applications.'' *React. Funct. Polym.*, **71** (2) 148–154 (2011)
47. Dunkers, J, Zarate, EA, Ishida, H, ''Crystal Structure and Hydrogen-Bonding Characteristics of *N*,*N*-Bis(3,5-dimethyl-2-hydroxybenzyl)methylamine, A Benzoxazine Dimer.'' *J. Chem. Phys.*, **100** (32) 13514–13520 (1996)
48. Tatiya, PD, Hedaoo, RK, Mahulikar, PP, Gite, VV, ''Novel Polyurea Microcapsules Using Dendritic Functional Monomer: Synthesis, Characterization, and Its Use in Self-healing and Anticorrosive Polyurethane Coatings.'' *Ind. Eng. Chem. Res.*, **52** (4) 1562–1570 (2013)
49. Mishra, AK, Narayan, R, Raju, K, Aminabhavi, TM, ''Hyperbranched Polyurethane (HBPU)-Urea and HBPU-Imide Coatings: Effect of Chain Extender and NCO/OH Ratio on Their Properties.'' *Prog. Org. Coat.*, **74** (1) 134–141 (2012)
50. Wang, H, Niu, Y, Fei, G, Shen, Y, Lan, J, ''In-Situ Polymerization, Rheology, Morphology and Properties of Stable Alkoxysilane-Functionalized Poly (Urethane-Acrylate) Microemulsion.'' *Prog. Org. Coat.*, **99** 400–411 (2016)
51. Feng, Y, Liang, H, Yang, Z, Yuan, T, Luo, Y, Li, P, Yang, Z, Zhang, C, ''A Solvent-Free and Scalable Method to Prepare Soybean-Oil-Based Polyols by Thiol-Ene Photo-Click Reaction and Biobased Polyurethanes Therefrom.'' *ACS Sustain. Chem. Eng.*, **5** (8) 7365–7373 (2017)
52. Wu, Y, Duan, H, Yu, Y, Zhang, C, ''Preparation and Performance in Paper Coating of Silicone-Modified Styrene–Butyl Acrylate Copolymer Latex.'' *J. Appl. Polym. Sci.*, **79** (2) 333–336 (2001)
53. Chen, A, Yao, C, Zeng, S, Yi, C, Xu, Z, ''Preparation and Properties of Hyperbranched Polyurethanes via Oligomeric $A_2 + bB_2$ Approach.'' *Polym. Bull.*, **61** (3) 363–371 (2008)
54. Deka, H, Karak, N, ''Bio-based Hyperbranched Polyurethanes for Surface Coating Applications.'' *Prog. Org. Coat.*, **66** (3) 192–198 (2009)
55. Dai, J, Liu, X, Ma, S, Wang, J, Shen, X, You, S, Zhu, J, ''Soybean Oil-Based UV-Curable Coatings Strengthened by Crosslink Agent Derived from Itaconic Acid Together with 2-Hydroxyethyl Methacrylate Phosphate.'' *Prog. Org. Coat.*, **97** 210–215 (2016)